

Substrate-Integrated Coaxial Bandpass Filters With Symmetrical Quasi-Absorptive Response

Dimitra Psychogiou¹ and Roberto Gómez-García²

Department of Electrical, Computed and Energy Engineering, University of Colorado Boulder, Boulder, CO, USA

Department of Signal Theory and Communications, University of Alcalá, Alcalá de Henares, Spain

Abstract

This paper discusses a new class of substrate-integrated coaxial (SIC) resonator-based bandpass filters (BPFs) with symmetrical/two-port quasi-reflectionless behavior and quasi-elliptic-type power transmission response. The proposed quasi-absorptive SIC BPF concept is based on in-series-cascaded two-pole/one-transmission-zero (TZ) BPF modules that are resistively terminated with first-order bandstop filtering sections. High levels of filtering selectivity and low in-band insertion loss are obtained by using high-quality-factor coaxial-cavity resonators and a mixed electromagnetic (EM) inter-resonator coupling. The enabling capabilities of the engineered quasi-absorptive SIC-based BPF concept are discussed through various theoretical examples and the manufacturing and testing of an S-band prototype with the following performance metrics: center frequency of 3.75 GHz, minimum in-band insertion loss equal to 0.75 dB, 3-dB passband bandwidth (BW) of 540 MHz, and 10-dB-referred quasi-reflectionless BW equal to 1.93 GHz.

1 Introduction

Emerging wireless communication systems and, in particular, those aimed to serve the next era of 5G and Internet-of-Things (IoT) devices are increasingly calling for multi-functional and high-performance RF transceivers. In particular, their RF front-ends will need to support a large number of applications/standards with diverse requirements in terms of frequency of operation, bandwidth (BW), and signal-to-noise ratio (SNR) while exhibiting small size, weight, and power (SWaP). In order to increase the receiver sensitivity, a plethora of bandpass and bandstop filters are typically incorporated in the receiver RF front-end chain with the purpose of suppressing external interference. Furthermore, the inter-block reflections that desensitize the active stages are cancelled through the use of resistively-terminated circulators/isolators or resistively-terminated diplexers [1]-[3]. However, these solutions are large in size due to the need for non-reciprocal ferrite-based materials that require external magnetic biasing.

To reduce the RF front-end size while enhancing its robustness to inter-block RF power reflections, reflection cancellation methods that do not rely on ferrite-based components—i.e., circulators or isolators—are currently being explored [3]-[10]. They are based on reflectionless

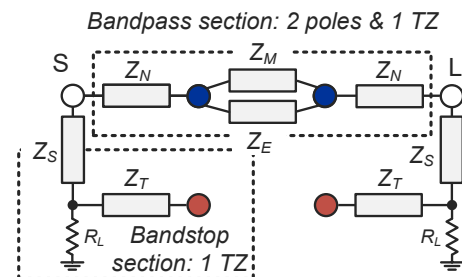


Figure 1. Block diagram of the quasi-absorptive BPF module that comprises a bandpass section and two resistively-terminated bandstop sections. The bandpass section is shaped by two resonators and a mixed EM coupling (shaped by the electric coupling inverter Z_E and the magnetic coupling inverter Z_M) and exhibits at two-pole/one-TZ response. The bandstop section consists of a first-order resistively-terminated bandstop filter and absorbs the reflected RF signal energy in the stopband. White circles: source and load. Blue and red circles resonators. Grey rectangles: impedance inverters.

or quasi-absorptive bandpass/bandstop filters that allow for reflection cancellation in both their passband and stopband regions by absorbing the non-transmitted/reflected RF signal energy within their volume. Illustrative examples of these concepts include lumped-element [3]-[6], [9] and planar high-pass/low-pass or bandpass/bandstop complementary-diplexer-based single-band and multi-band configurations [3], [8]. However, they are only able to perform the reflection-cancellation function at one of their ports, they exhibit low-quality-factor (Q , around 20-100) responses, and are mostly suitable for low-frequency applications. Furthermore, a large number of these concepts [4]-[6] relies on specific component values and tightly-coupled elements, which makes them hard to realize with commercial off-the-shelf components and require advanced manufacturing processes.

To address the aforementioned limitations, this paper focuses on the design and the practical development of a new class of high- Q quasi-absorptive bandpass filters (BPFs) with highly-selective power transmission response and symmetrical reflection cancellation. As opposed to conventional planar/lumped-element-based integration schemes, the focus of this work is on new design/integration alternatives using substrate-integrated coaxial (SIC) resonators and on the realization of highly-selective filtering transfer functions by incorporating

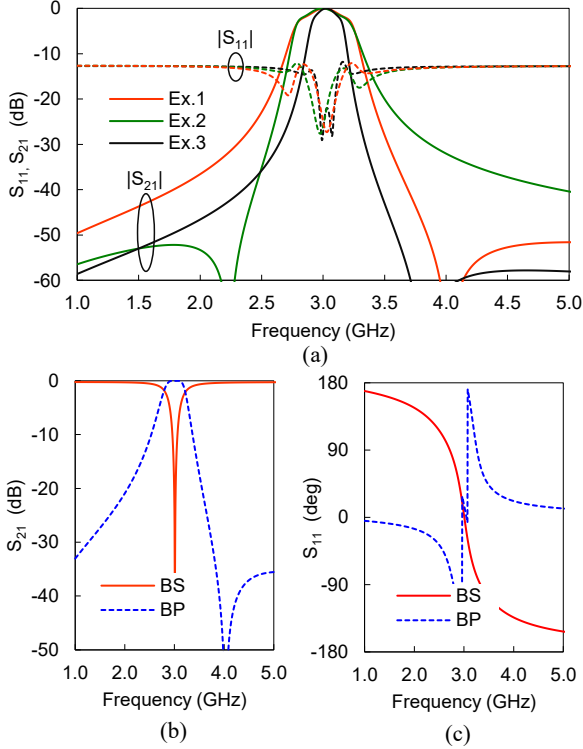


Figure 2. Theoretical power transmission and reflection responses of the quasi-absorptive BPF module in Figure 1 for a passband centered at 3 GHz. The illustrated responses were obtained with linear simulations using ideal inverters (normalized values to the port reference impedance are listed in Table 1) and parallel LC resonators. (a) Simulated examples showing how the mixed EM coupling can control the location of the TZ and how alternative BW states can be obtained. (b) and (c) Power transmission response of the BP and the BS sections of the quasi-absorptive BPF Example 1 in terms of amplitude and phase.

mixed-electromagnetic (EM) coupling between its constituent in-line resonators. Scalability of the proposed filter principle to high-order quasi-elliptic-type transfer functions is also shown. Lastly, the practical validation of the concept is reported in terms of EM analysis and the manufacturing and testing of a SIC-based BPF prototype.

2 Theoretical foundations

The operating principles of the suggested symmetrical quasi-reflectionless BPF concept are illustrated in the block diagram in Figure 1 and the theoretical power transmission and reflection responses in Figure 2. As shown, the proposed filter comprises four resonators (blue and red circles) and eight inverters (rectangles) that are arranged in a bandpass (BP) section and two resistively-terminated bandstop (BS) sections. The BP section consists of two resonators (blue circles) and a mixed EM coupling scheme (in parallel cascaded impedance inverters Z_M and Z_E with opposite phase response) that contribute to the overall power transmission response of the filter with two in-band poles and one transmission zero (TZ). Whereas the location of the poles is controlled by the resonant frequency of the

Table 1. Normalized impedance inverter values for the examples shown in Figure 1 and 2.

Example	1	2	3
Z_N	2.5	2.5	3.2
Z_M	2.5	4.3	3.8
Z_E	4.3	2.5	6.4
Z_S	3	3	2.2
Z_T	6	6	5.7
R_L	14.8	14.8	8

resonators and magnitude of the EM coupling at the center frequency of the passband f_{cen} , the location of the TZ is set at a frequency f_{TZ} where the mixed EM coupling is zero using (1).

$$f_{TZ} = f_{cen} \sqrt{\frac{Z_M}{Z_N}} \quad (1)$$

The reflection-cancellation process is performed by connecting first-order resistively-terminated BS sections at the input and output ports of the BP section. In this manner, the reflected RF signal energy in the out-of-band regions of BP section (i.e., frequencies at which it is highly reactive) is absorbed at the resistive terminations of the BS sections.

To better explain the operating capabilities of the proposed quasi-reflectionless BPF concept with TZs in its out-of-band response, various theoretical examples are shown in Figures 2 and 3. All examples have been performed for a center frequency of 3 GHz and using ideal impedance inverters (values listed in Table 1) and parallel LC resonators. It should be noticed that the resonator elements ($L=1.65$ nH and $C=1.7$ pF) are selected so that they correspond to the actual inductance/capacitance values that can be obtained with capacitively-loaded SIC-based resonators using the design process in [10].

Figure 2 (a) demonstrates the two-pole/one-TZ response of the quasi-absorptive BPF module in Figure 1 for different values of the coupling between its constituent resonators. As shown, the TZ can be either set above (Example 1) or below (Example 2) the BPF passband by controlling the amount of the electric (set by Z_E) and magnetic (set by Z_M) coupling between the resonators of the BP section. Larger magnetic coupling results in TZs at the upper side of the passband whereas larger electric coupling moves the TZ below the passband. As also shown at the same figure, both wide and narrow bandwidth (BW) responses can be obtained (see Examples 1 and 3) with the proposed topology as long as the power transmission response of its constituent sections are complementary in terms of amplitude and phase. This is confirmed in Figure 2(b) in which the responses of the BP and the BS sections are plotted for the first example in Figure 2(a).

The symmetrical quasi-reflectionless BPF concept can be extended to high-order transfer functions by readily cascading in series multiple two-pole/one-TZ modules. This is shown in the block diagram in Figure 3(a) for the

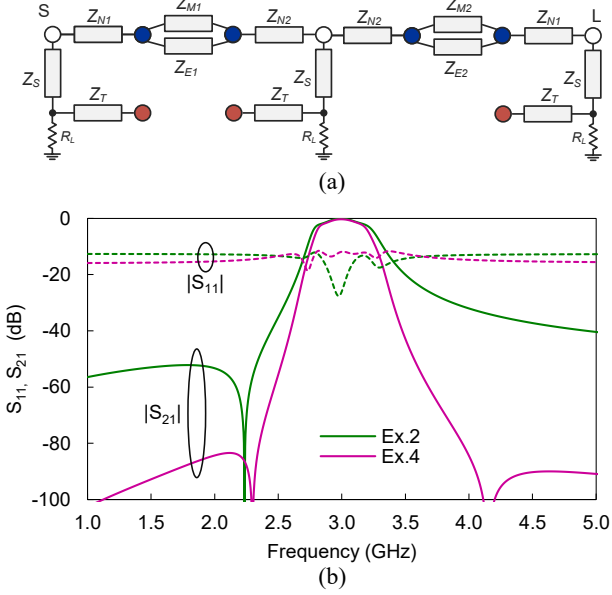


Figure 3. Block diagram and example power transmission and reflection responses of a high-order quasi-absorptive BPF that comprises two in-series-cascaded modules. (a) Block diagram. (b) S-parameters of the high-order module and one of its constituent modules (TZ on the left).

example case of a passband shaped by four poles and two TZs. The TZs can be either set symmetrically or asymmetrically around the passband and further enhance the transfer function selectivity. To illustrate the high-selectivity capabilities of the concept, an example case of a quasi-absorptive bandpass transfer function with symmetrically-allocated TZs is depicted in Figure 3(b), alongside a comparison with the power transmission response of one of its modules. It is apparent that higher selectivity or additional TZs can be obtained by cascading in series additional modules.

3 Substrate-Integrated Coaxial Resonator-Based Integration Concept

To validate the operating principles of the devised quasi-reflectionless BPF concept, a two-pole/one-TZ BPF prototype was designed, manufactured, and measured at the S-band for a center frequency of 3.65 GHz and BW of 460 MHz. For its practical development, miniaturized capacitively-loaded SIC resonators were employed as, for example, the ones shown in [10]. For their design, a Rogers TMM 3 substrate (dielectric thickness $h=3.175$ mm, relative permittivity $\epsilon_r=3.32$, and dielectric loss tangent $\tan\delta=0.002$) was used. The 3D EM model of each of the BP and BS sections, along with their corresponding EM responses, are shown in Figure 4. The BP section that is depicted in Figure 4(a) is materialized with two capacitively-loaded coaxial resonators that are coupled with a mixed EM coupling scheme that is shaped by an evanescent-mode waveguide section (magnetic coupling Z_M) and a capacitive gap (electric coupling Z_E) between the two posts of the coaxial resonators. Its magnitude is controlled by the resonator spacing d and the capacitive gap g . The external coupling (inverter Z_N in Figure 1) is made

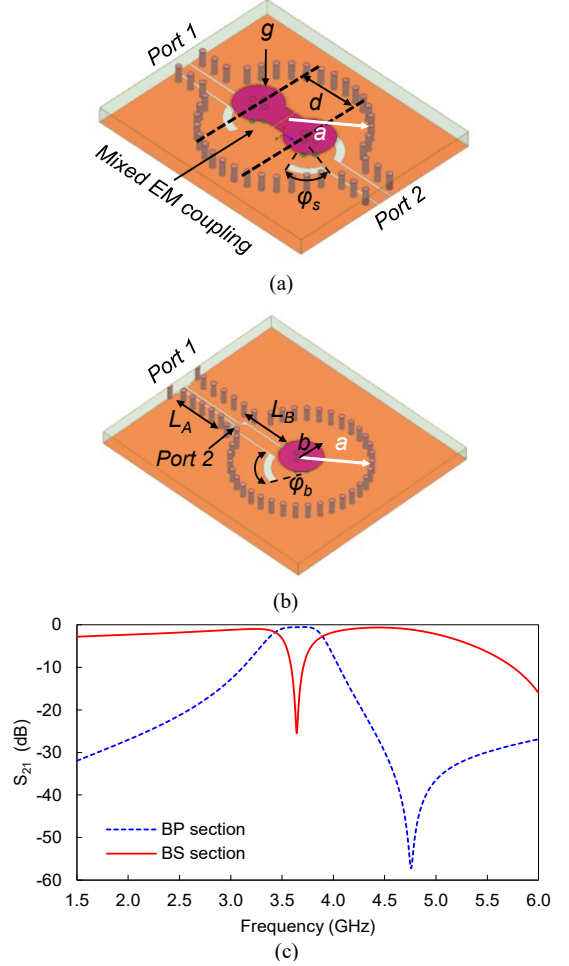


Figure 4. Conceptual drawing and 3D model of the BP and BS sections and their power transmission responses. (a) 3D model of the BP section. (b) 3D model of the BS section. (c) Power transmission responses. The indicated dimensions are: $g=0.3$ mm $b=4$ mm, $a=12.5$ mm, $d=10.7$ mm, $\phi_s=58^\circ$, $\phi_b=65^\circ$, $L_A=12.5$ mm, and $L_B=8.7$ mm.

with slot openings in the bottom metallization layer and is controlled by the slot angle ϕ_b . The BS section in Figure 4(b) is made from a resistively-terminated first-order bandstop filter. After designing each of the individual filter sections, the 3D model of the filter was constructed in ANSYS HFSS and optimized to compensate the parasitics at the connecting junctions. The final EM model and its corresponding EM response are respectively shown in Figures 5(a) and 6. As shown, the resistive BS-section terminations absorb the reflected RF signal energy in the stopband regions of the BP section.

4 Experimental Validation

The manufactured prototype of the two-pole/one-TZ SIC resonator-based BPF concept was manufactured using in-house PCB manufacturing and is shown in Figure 5(b). Its S-parameters were characterized with a N5224A power network analyzer (PNA) from Keysight and are depicted in Figure 6. Their main metrics are summarized as follows: center frequency of 3.75 GHz, minimum in-band insertion loss of 0.75 dB, 3-dB passband BW equal to 540 MHz, 10-

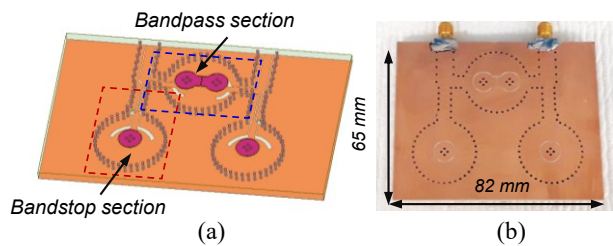


Figure 5. (a) 3D model of the two-pole/one-TZ SIC-resonator-based BPF. (b) Manufactured prototype.

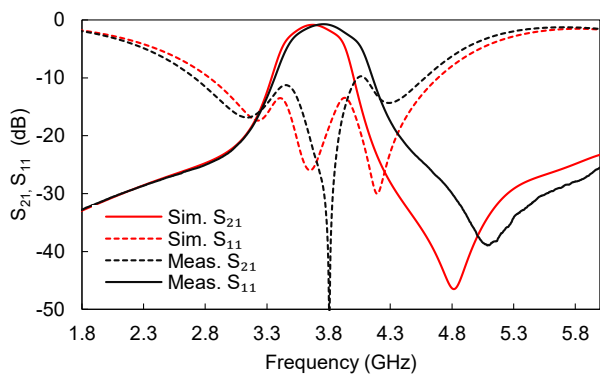


Figure 6. RF-measured and EM-simulated power transmission and reflection responses of the developed SIC-resonator-based quasi-absorptive BPF prototype.

dB-referred quasi-reflectionless BW of 1.93 GHz. A comparison between the RF-measured and EM simulated responses is also shown at the same figure, which as proven are in a good agreement. The slight discrepancies in the RF-measured response are due to manufacturing tolerances of our in-house PCB manufacturing process.

4 Conclusion

This paper explored the design and practical validation of a new class of substrate-integrated waveguide BPFs with symmetrical quasi-absorptive response. The proposed filter concept is based on capacitively-loaded coaxial resonators that allow for high Q and size compactness. The quasi-absorptive behavior is obtained by loading the input/output ports of a two-pole/one-TZ BPF with resistively-terminated first-order BS sections. High levels of selectivity are obtained by incorporating mixed EM coupling in-between the resonators of the BP section. Extension of this concept to higher-order filter topologies by cascading in series multiple of the two-pole/one-TZ modules was also discussed. The operating principles of the proposed quasi-absorptive SIC-based BPF concept were validated experimentally at the S-band.

6 Acknowledgements

This work has been supported in part by the National Science Foundation under award number 1731956.

7 References

1. Mini-Circuits, "Reflectionless filters improve linearity and dynamic range," *Microwave Journal*, **58**, 8, August 2015, pp. 42-50.
2. K. A. Gallager, "Harmonic radar: Theory and applications to nonlinear target detection, tracking, imaging and classification," Ph.D. dissertation, Dept. Elect. Eng., Pennsylvania State Univ., State College, PA, USA, Dec. 2015.
3. D. Psychogiou and R. Gómez-García, "Reflectionless adaptive RF filters: bandpass, bandstop, and cascade designs," *IEEE Trans. Microw. Theory Techn.*, **65**, 11, November 2017, pp. 4593-4605, doi: 10.1109/TMTT.2017.2734086.
4. S.-W. Jeong T.-H. Lee, and J. Lee, "Frequency- and bandwidth-tunable absorptive bandpass filter," *IEEE Trans. Microw. Theory Techn.*, **67**, 6, June, 2019, pp. 2172-2180, doi: 10.1109/TMTT.2019.2914111.
5. M. A. Morgan and T. A. Boyd, "Theoretical and experimental study of a new class of reflectionless filter," *IEEE Trans. Microw. Theory Techn.*, **59**, 5, May 2011, pp. 1214-1221, doi: 10.1109/TMTT.2011.2113189.
6. M. A. Morgan and T. A. Boyd, "Reflectionless filter structures," *IEEE Trans. Microw. Theory Techn.*, **63**, no. 4, April 2015, pp. 1263-1271, doi: 10.1109/TMTT.2015.2403841.
7. R. Gómez-García, J.-M. Muñoz-Ferreras and D. Psychogiou, "High-order input-reflectionless bandpass/bandstop filters and multiplexers," *IEEE Trans. Microw. Theory Techn.*, **67**, 9, September 2019, pp. 3683-3695, doi: 10.1109/TMTT.2019.2924975.
8. R. Gómez-García, J.-M. Muñoz-Ferreras, and D. Psychogiou, "Symmetrical quasi-absorptive RF bandpass filters," *IEEE Trans. Microw. Theory Techn.*, **67**, no. 4, April 2019, pp. 1472-1482, doi: 10.1109/TMTT.2019.2895531.
9. D. Psychogiou and R. Gómez-García, "Symmetrical quasi-reflectionless SAW-based bandpass filters with tunable bandwidth," *IEEE Microw. Wireless Comp. Lett.*, **29**, 7, July 2019, pp. 447-449, doi: 10.1109/LMWC.2019.2918413.
10. A. Anand and X. Liu, "Substrate-integrated coaxial-cavity filter with tunable center frequency and reconfigurable bandwidth," in *Proc. IEEE 15th Wireless Microw. Technol. Conf.*, Tampa, FL, USA, June 6, 2014, pp. 1-4, doi: 10.1109/WAMICON.2014.6857772.